Supplementary Information

Combined Influence of QM Methods, Active Space Size, Franck-Condon Approximation, Herzberg-Teller Effect and Duschinsky Effect on Vibrationally Resolved Electronic Spectra: Insights from Firefly Oxyluciferin

Shuangqi Pi[a,&], *Cheng Peng*[b,&], Haibo Ma[b,*] and *Ya-Jun Liu*[a,c,*]

[a] Center for Advanced Materials Research, Beijing Normal University, Zhuhai 519087, China.

[b] Key Laboratory for Colloid and Interface Chemistry, Ministry of Education, School of Chemistry and Chemical Engineering, Shandong University, 72 Binhai Road, Qingdao 266237, China

[c] Key Laboratory of Theoretical and Computational Photochemistry, Ministry of Education, College of Chemistry, Beijing Normal University, Beijing 100875, China.

[&] These authors contributed equally to this work and should be considered co-first authors

*** Correspondence:**
Corresponding Author's E-mail: haibo.ma@sdu.edu.cn, yajun.liu@bnu.edu.cn

Contents

Additional Figures and Tables S3

Table S1. The comparison of (TD) CAM-B3LYP/aug-cc-pVTZ and (TD) ωB97X-D/aug-cc-pVTZ calculated vertical excitation energies T_v, emission energies T_e, adiabatic transition energies E_{ad} and 0-0 transition energies E_{ad}. S3

Table S2. The (TD) CAM-B3LYP/aug-cc-pVTZ optimized main geometrical parameters (in Å) of the S_0 and S_1 states of the OL^-. S4

Table S3. The CASSCF/ANO-RCC-VDZP optimized main geometrical parameters (in Å) of the S_0 and S_1 states of the OL^-. S4

Figure S1. The active orbitals of the phenolate-enol form of OL^-. S5

Figure S2. The active orbitals of the phenolate-keto form of OL^- S7

Figure S3. The active orbitals of the meo-OL^-.....S10

Figure S4. The active orbitals of the dm-OL^- S13

Figure S5. The entanglements of the phenolate-keto form of OL^- in the S_0 and S_1 states S16

Figure S6. The entanglements of meo-OL^- in the S_0 and S_1 states S17

Figure S7. The entanglements of dm-OL^- in the S_0 and S_1 states S17

Figure S8. Scaled displacement vectors of the relevant vibrational modes in the S_1 state for phenolate-enol. S18

Figure S9. Scaled displacement vectors of the relevant vibrational modes in the S_1 state for phenolate-keto S18

Figure S10. Scaled displacement vectors of the relevant vibrational modes in the S_1 state for meo-OL^-. S18

Figure S11. Scaled displacement vectors of the relevant vibrational modes in the S_1 state for dm-OL^- ...S18

Figure S12. The duschinsky matrix of S_1-state and S_0-state normal modes. S19

Figure S13. The comparison of absorption spectra simulated by AS model and AH model to consider the influence of Duschinsky effect. S20

Figure S14. The comparison of absorption spectra simulated by AH model to consider the influence of Herzberg-Teller effect.....S21

Figure S15. Scaled displacement vectors of the relevant vibrational modes in the S_0 state for phenolate-enol S21

Figure S16. Scaled displacement vectors of the relevant vibrational modes in the S_0 state for phenolate-keto S22

Figure S17. Scaled displacement vectors of the relevant vibrational modes in the S_0 state for meo-OL^- .S22

Figure S18. Scaled displacement vectors of the relevant vibrational modes in the S_0 state for dm-OL^- ...S22

Figure S19. The comparison of fluorescence spectra simulated by AS model and AH model to consider the influence of Duschinsky effect. S23

Figure S20. The comparison of fluorescence spectra simulated by AH model to consider the influence of Herzberg-Teller effect. S24

The XYZ Cartesian Coordinates of Key Structures Reported (unit: Ångstrom) S25

Table S1. The vertical excitation energies T_v (in eV), emission energies T_e (in eV), adiabatic transition energies E_{ad} (in eV) and 0-0 transition energies E_{ad} (in eV) calculated at (TD) CAM-B3LYP/aug-cc-pVTZ and (TD) ωB97X-D/aug-cc-pVTZ level in gas phase. The values in parentheses represent oscillator strength (*f*). The absorption and emission maxima of gaseous OL^- and derivatives at 100 K from experiment.

species		exp. max	CAM-B3LYP	ωB97X-D
phenolate-enol	T_v		2.70 (0.690)	2.75 (0.685)
	T_e	2.21	2.53 (0.668)	2.55 (0.679)
	E_{ad}	-	2.62	2.65
	E_{0-0}	-	2.55	2.58
phenolate-keto	T_v	-	2.71 (0.819)	2.71 (0.805)
	T_e	2.09~2.08	2.53 (0.697)	2.54 (0.698)
	E_{ad}	-	2.63	2.62
	E_{0-0}	-	2.56	2.56
meo-OL^-	T_v	2.21	2.70 (0.693)	2.74 (0.690)
	T_e	2.19~2.20	2.52 (0.677)	2.53 (0.689)
	E_{ad}	-	2.61	2.64
	E_{0-0}	2.21	2.54	2.58
dm-OL^-	T_v	2.10~2.13	2.70 (0.857)	2.69 (0.843)
	T_e	2.06~2.08	2.52 (0.733)	2.52 (0.735)
	E_{ad}	-	2.61	2.61
	E_{0-0}	-	2.54	2.55

Table S2. The (TD) CAM-B3LYP/aug-cc-pVTZ optimized main geometrical parameters (in Å) of the S_0 and S_1 states of the OL^- (Figure 1).

species	state	O10′—C6′	O11′—C4	N3′—C2′	N3—C2	C2′—C2
phenolate-enol	S_0	1.250	1.360	1.299	1.307	1.429
	S_1	1.249	1.364	1.328	1.334	1.410
phenolate-keto	S_0	1.243	1.211	1.316	1.302	1.405
	S_1	1.247	1.218	1.325	1.312	1.418
dm-OL^-	S_0	1.250	1.352	1.298	1.309	1.429
	S_1	1.249	1.355	1.328	1.337	1.408
meo-OL^-	S_0	1.243	1.212	1.316	1.305	1.405
	S_1	1.247	1.220	1.325	1.315	1.418

Table S3. The CASSCF/ANO-RCC-VDZP optimized main geometrical parameters (in Å) of the S_0 and S_1 states of the OL^- (Figure 1).

species	state	O10′—C6′	O11′—C4	N3′—C2′	N3—C2	C2′—C2
phenolate-enol	S_0	1.236	1.352	1.306	1.300	1.428
	S_1	1.245	1.360	1.312	1.337	1.417
phenolate-keto	S_0	1.228	1.204	1.324	1.299	1.398
	S_1	1.245	1.212	1.305	1.315	1.431
dm-OL^-	S_0	1.228	1.205	1.324	1.299	1.399
	S_1	1.245	1.214	1.305	1.315	1.432
meo-OL^-	S_0	1.236	1.348	1.305	1.302	1.429
	S_1	1.245	1.357	1.312	1.338	1.416

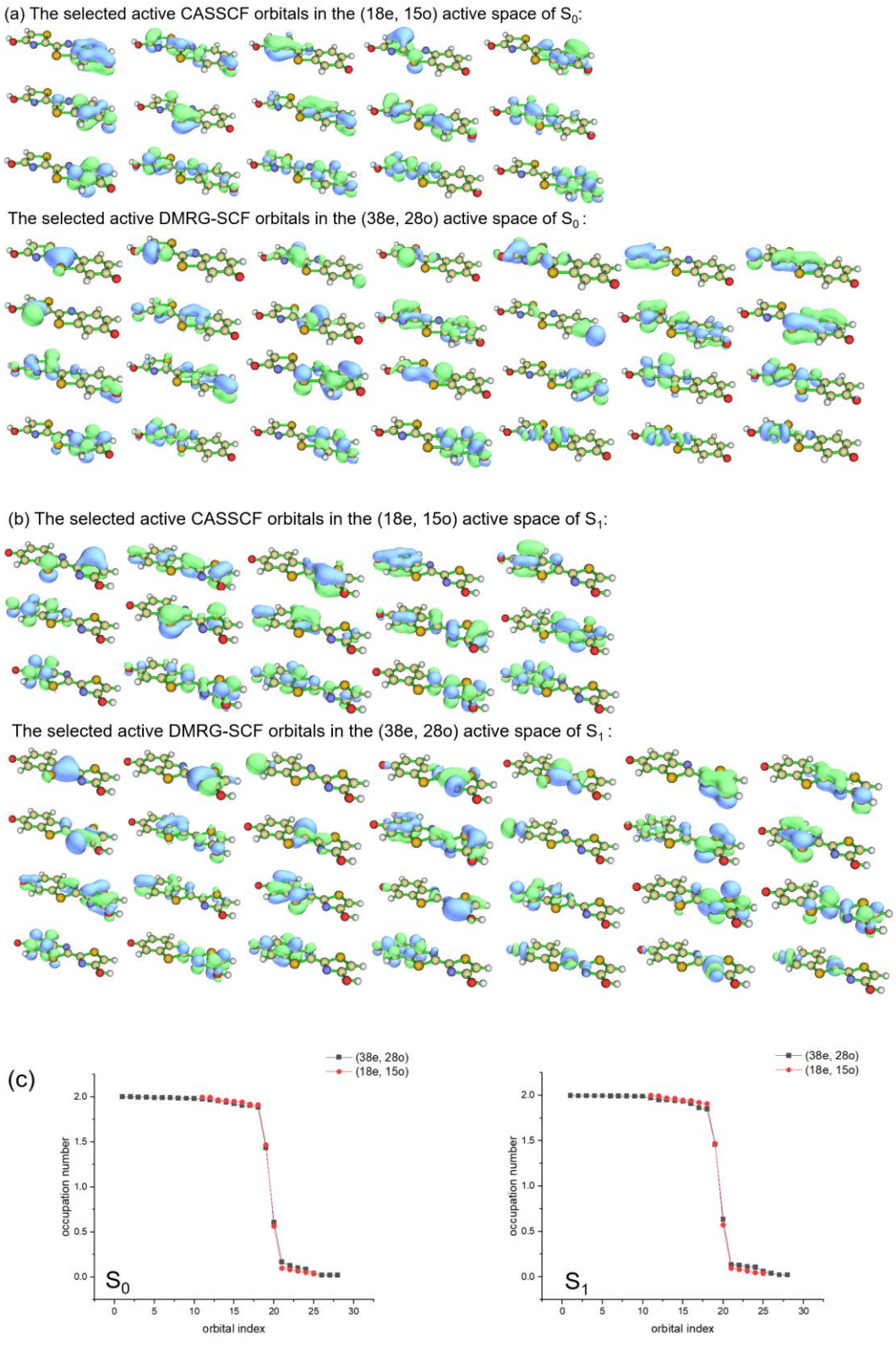

Figure S1. (a) The selected active orbitals of the phenolate-enol form of OL^- molecule in the S_0 state (isosurfaces at 0.05 a.u.) calculated using CASSCF in the (18e, 15o) active space and DMRG-SCF orbitals in the (38e, 28o) active space; (b) in the S_1 state; (c) the natural occupation number comparison with different active spaces.

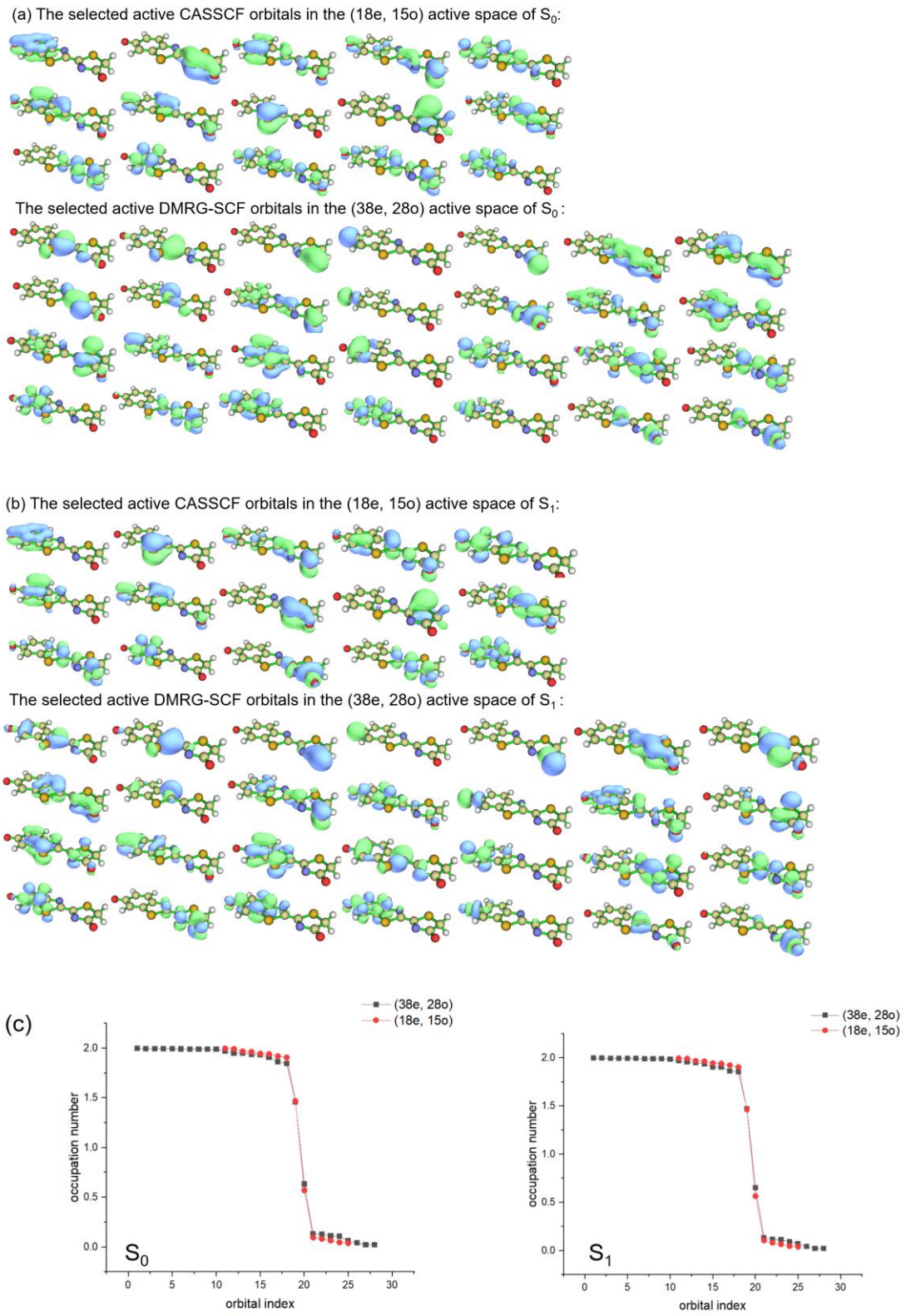

Figure S2. (a) The selected active orbitals of the phenolate-keto form of OL^- molecule in the S_0 state (isosurfaces at 0.05 a.u.) calculated using CASSCF in the (18e, 15o) active space and DMRG-SCF orbitals in the (38e, 28o) active space; (b) in the S_1 state; (c) the natural occupation number comparison with different active spaces.

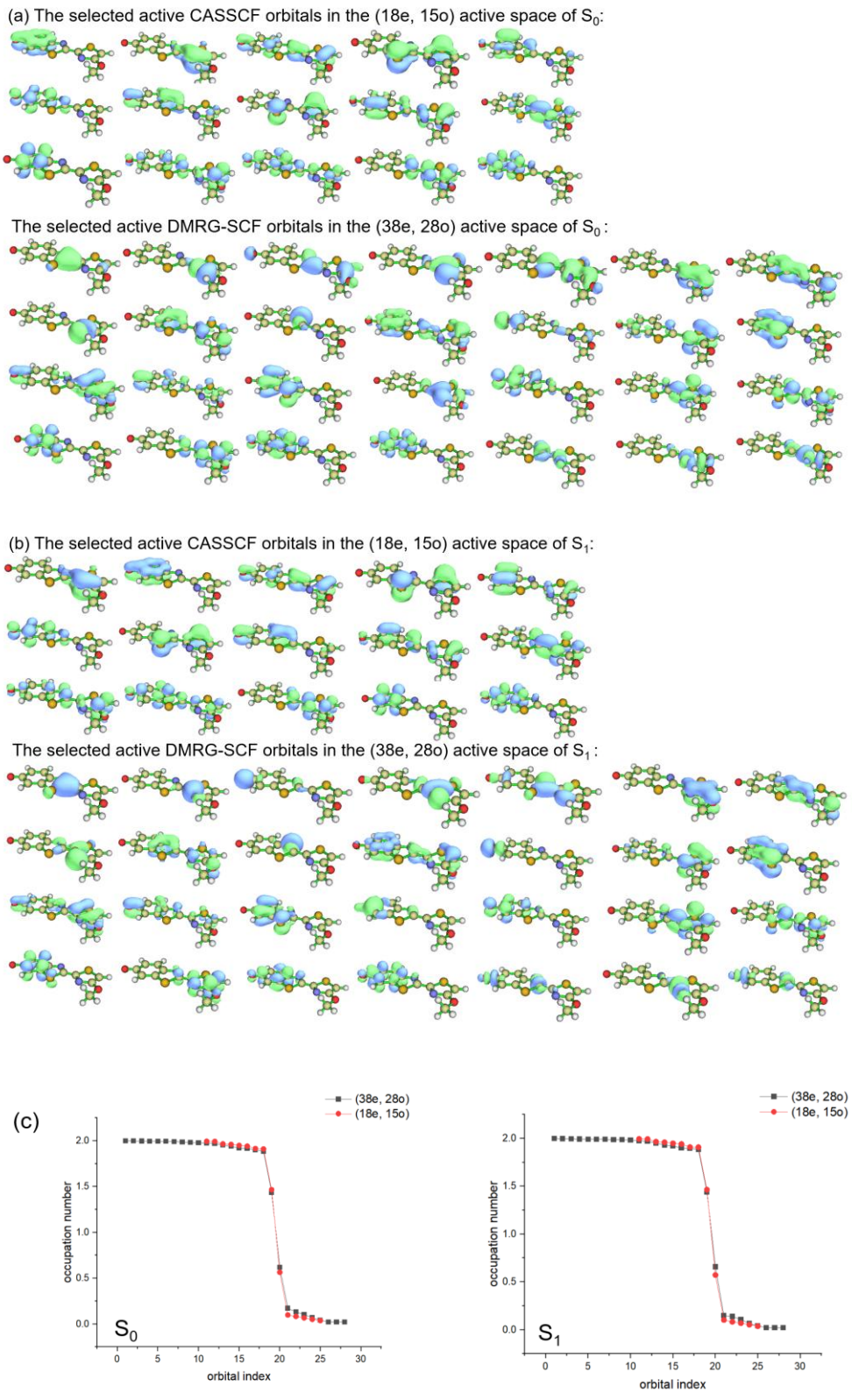

Figure S3. (a) The selected active orbitals of the meo-OL$^-$ molecule in the S_0 state (isosurfaces at 0.05 a.u.) calculated using CASSCF in the (18e, 15o) active space and DMRG-SCF orbitals in the (38e, 28o) active space; (b) in the S_1 state; (c) the natural occupation number comparison with different active spaces.

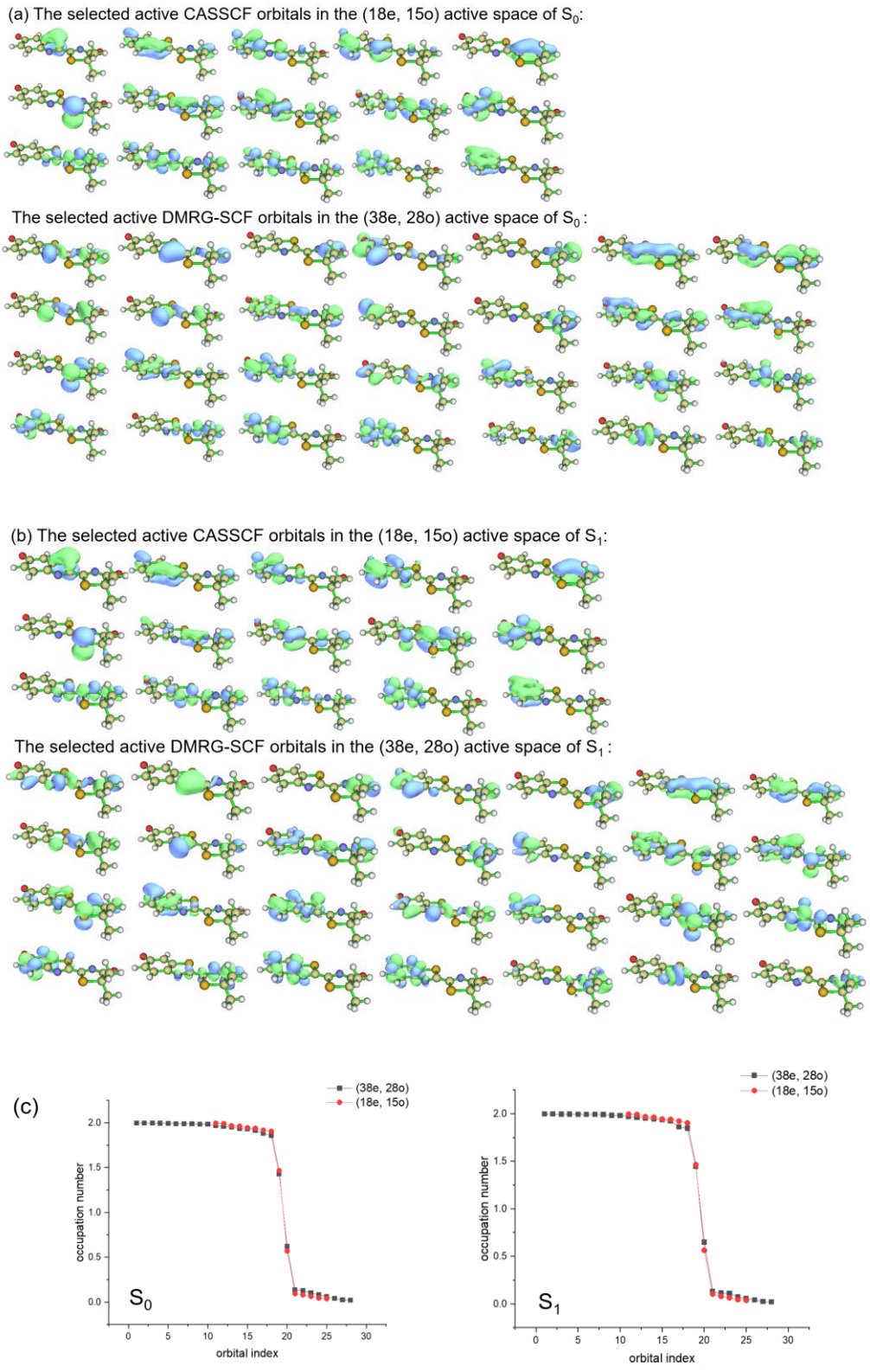

Figure S4. (a) The selected active orbitals of the dm-OL$^-$ molecule in the S_0 state (isosurfaces at 0.05 a.u.) calculated using CASSCF in the (18e, 15o) active space and DMRG-SCF orbitals in the (38e, 28o) active space; (b) in the S_1 state; (c) the natural occupation number comparison with different active spaces.

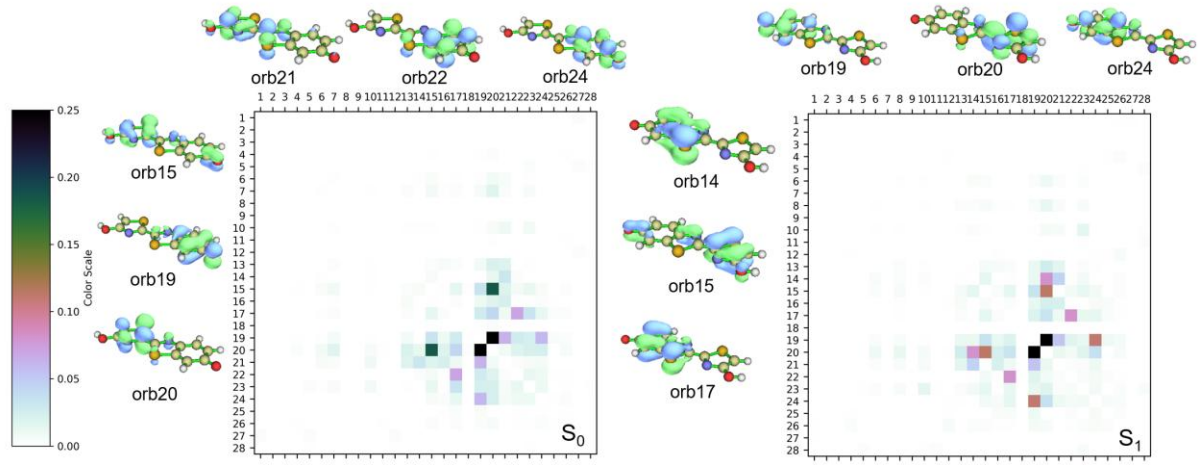

Figure S6. Illustrations of the entanglements of the phenolate-keto form of OL^- molecule in the S_0 (a) and S_1 (b) states, based on DMRG-SCF wave functions. The key entanglement orbitals are also highlighted.

The main entanglement in the S_0 state of the keto form is between orbital 19 and 20. Other important interactions include orbital 15 and 20. For the keto form species in the S_1 state, the most significant entanglement also takes place between orbital 19 and 20, with a less significant orbital pair 15 and 20, 19 and 24.

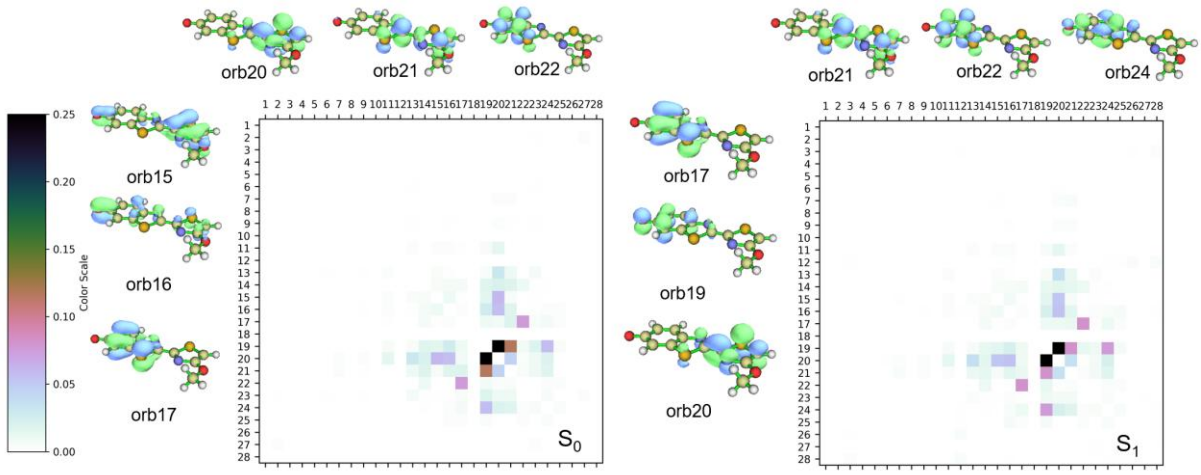

Figure S7. Illustrations of the entanglements of the meo-OL^- in the S_0 (a) and S_1 (b), based on DMRG-SCF wave functions. The key entanglement orbitals are also highlighted.

In the S_0 state of meo-OL^-, the predominant entanglement occurs between orbitals 19 and 20, while interactions between orbital pairs 20 and 21 are also notably stronger than other orbital pairs. In the S_1 state, the entanglement patterns are largely similar to those observed in the S_0 state.

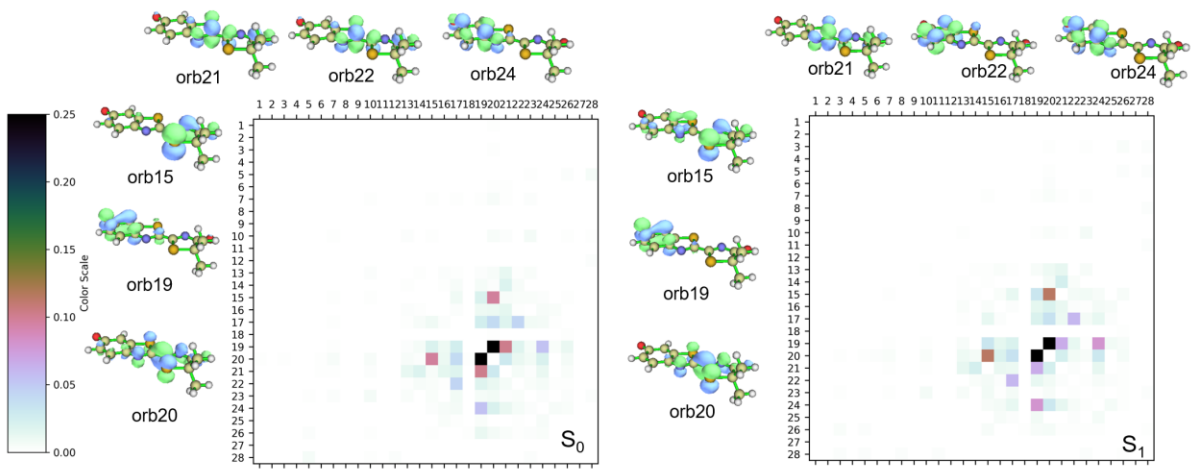

Figure S8. Illustrations of the entanglements of the dm-OL$^-$ in the S_0 (a) and S_1 (b), based on DMRG-SCF wave functions. The key entanglement orbitals are also highlighted.

The most significant entanglement in the S_0 state of dm-OL$^-$ occurs between orbitals 19 and 20, with a secondary entanglement between orbitals 15 and 20, followed by the entanglement between orbitals 19 and 21 as another notable interaction. In the S_1 state, the entanglement patterns exhibit similar trends to those in the S_0 state. However, while the locations of orbital entanglements are comparable, there are subtle differences in their intensities.

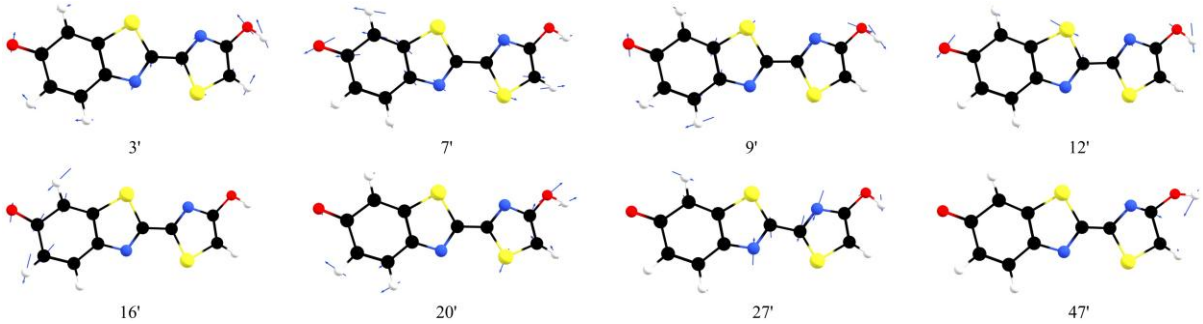

Figure S8. Scaled displacement vectors of the relevant vibrational modes in the S_1 state for phenolate-enol.

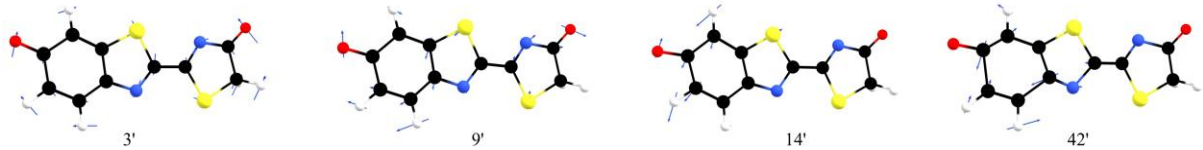

Figure S9. Scaled displacement vectors of the relevant vibrational modes in the S_1 state for phenolate-keto.

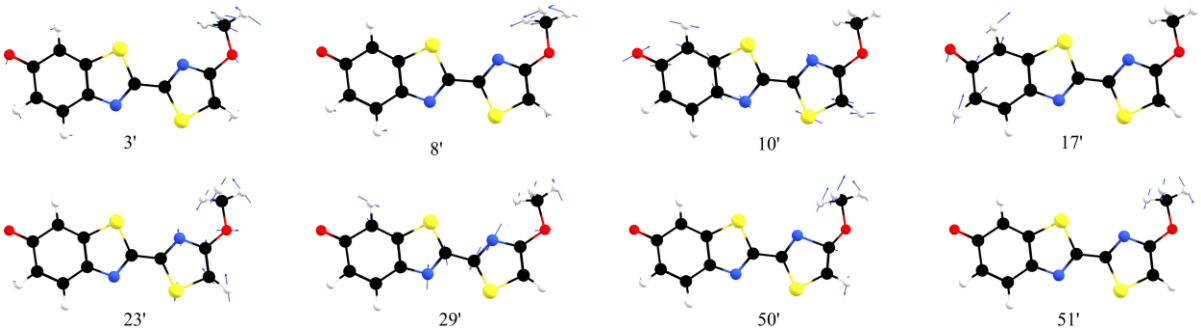

Figure S10. Scaled displacement vectors of the relevant vibrational modes in the S_1 state for meo-OL^-.

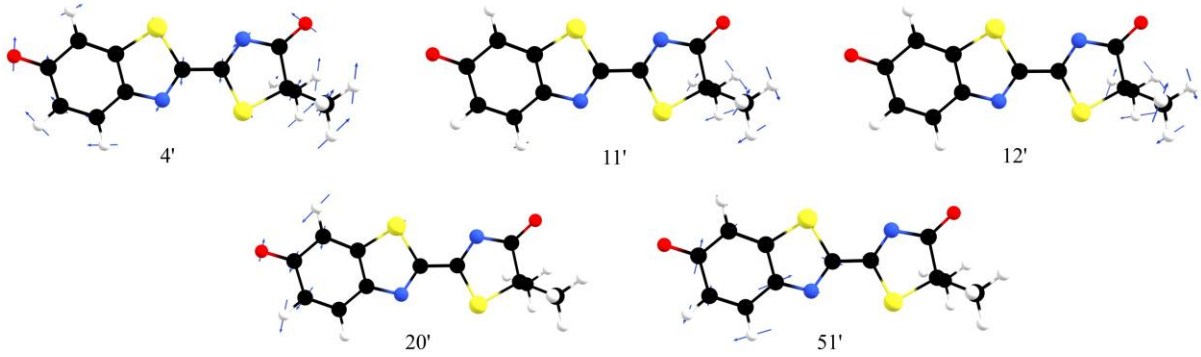

Figure S11. Scaled displacement vectors of the relevant vibrational modes in the S_1 state for dm-OL^-.

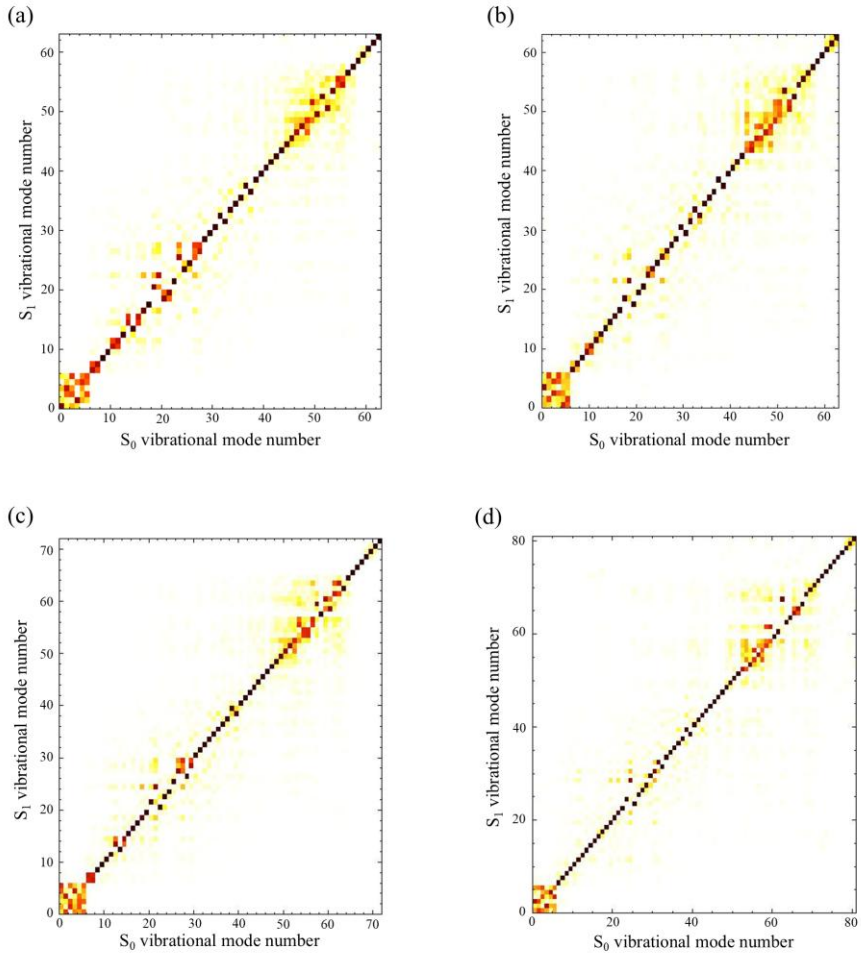

Figure S12. The duschinsky matrix of S_1-state and S_0-state normal modes for (a) phenolate-enol, (b) phenolate-keto, (c) meo-OL^- and (d) dm-OL^- calculated at the CAM-B3LYP/aug-cc-pVTZ level in gas.

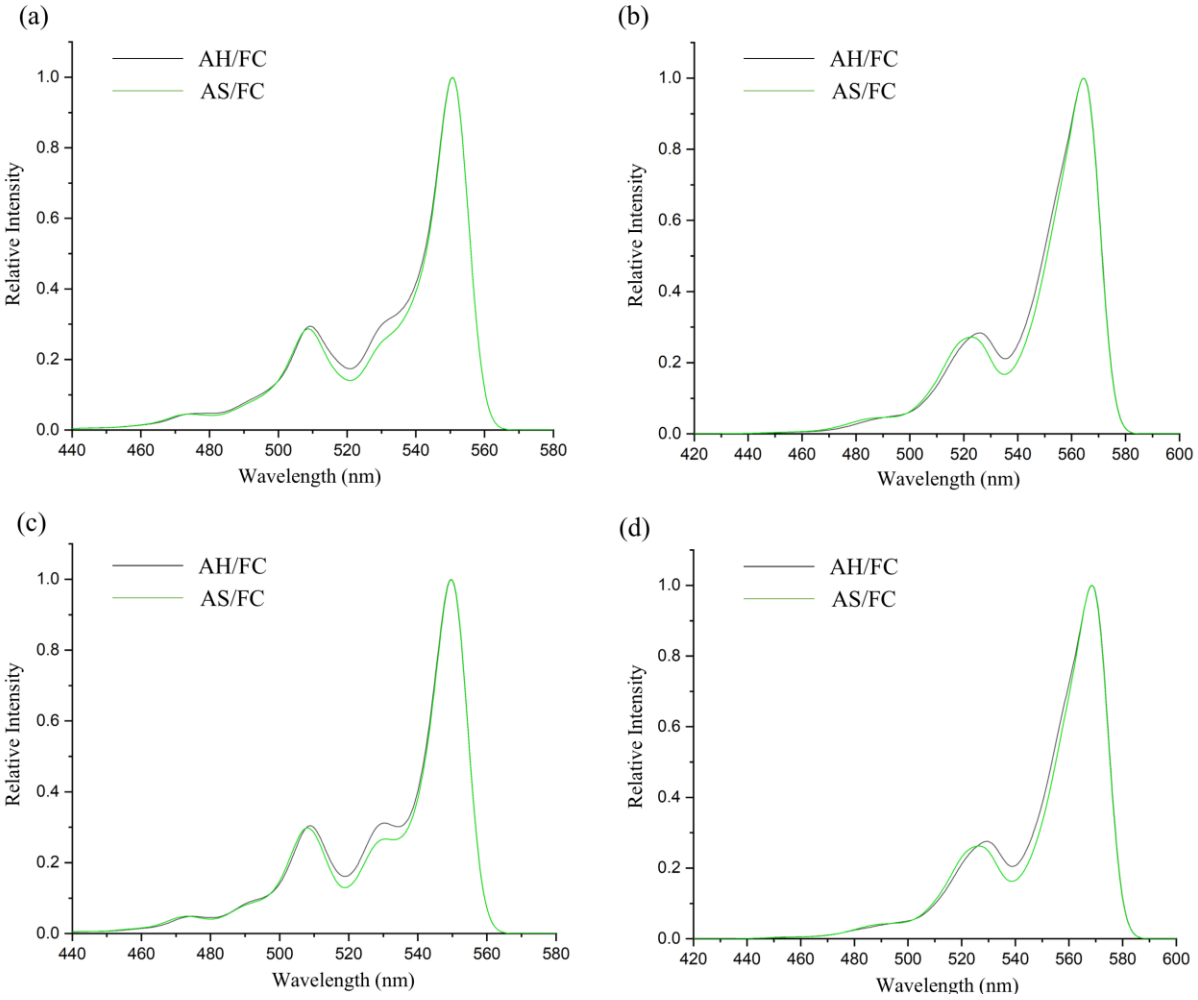

Figure S13. The comparison of absorption spectra of (a) phenolate-enol (b) phenolate-keto, (c) meo-OL^- and (d) dm-OL^- simulated by AS model (green line) and AH model (black line) to consider the influence of Duschinsky effect. Here, the absorption spectra simulated by the AS model is aligned with the spectra simulated by the AH model for ease of comparison.

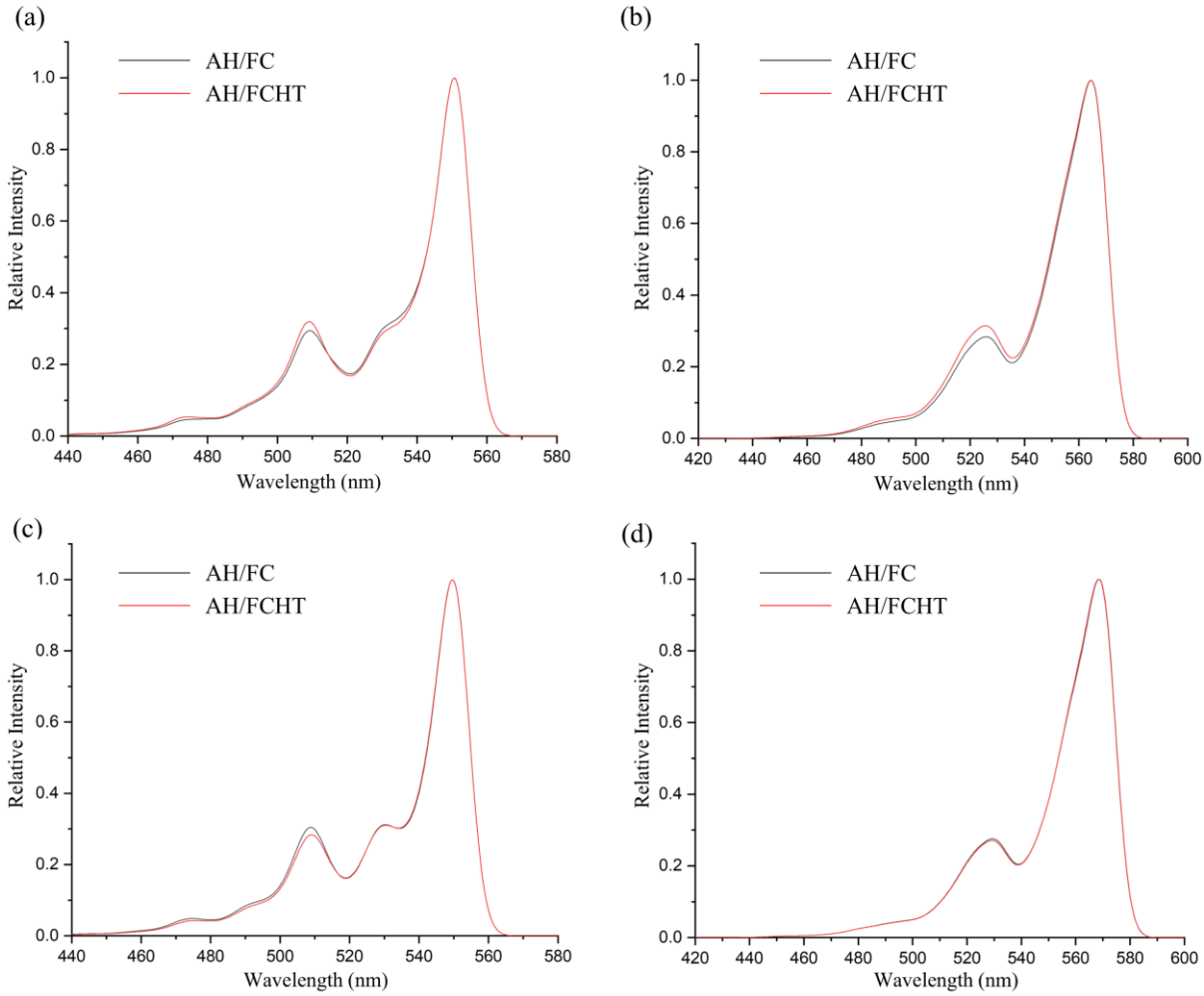

Figure S14. The comparison of absorption spectra of (a) phenolate-enol (b) phenolate-keto, (c) meo-OL^- and (d) dm-OL^- simulated by AH model to consider the influence of Herzberg-Teller effect. The black line represents that only FC effect is considered, while the red line represents that both FC and HT effects are considered.

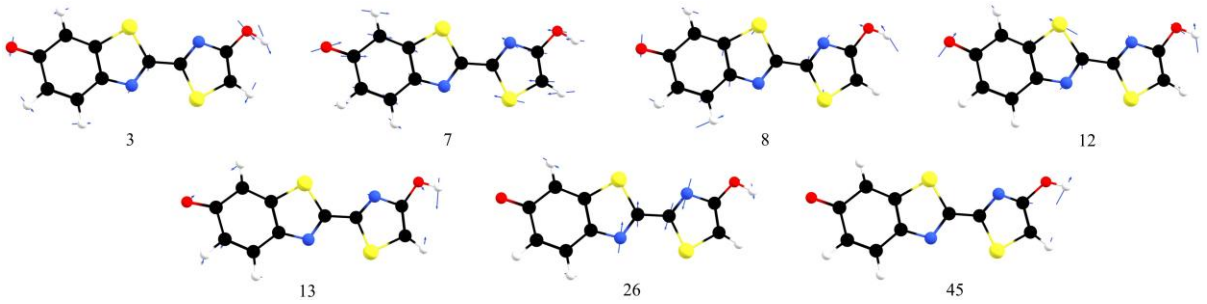

Figure S15. Scaled displacement vectors of the relevant vibrational modes in the S_0 state for phenolate-enol.

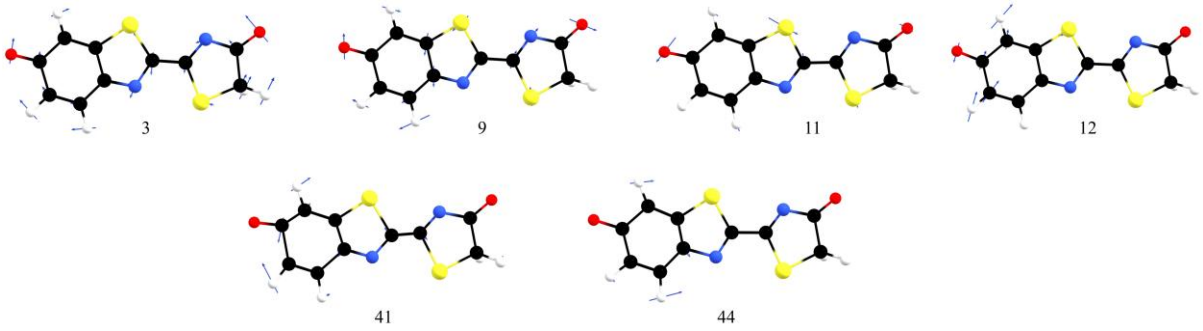

Figure S16. Scaled displacement vectors of the relevant vibrational modes in the S_0 state for phenolate-keto.

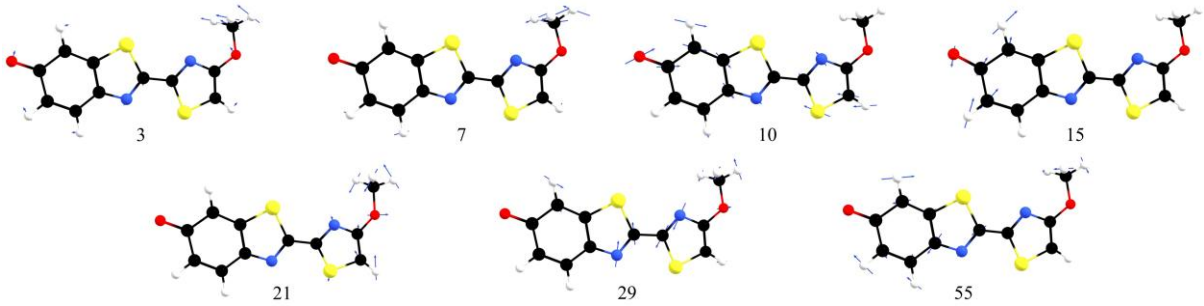

Figure S17. Scaled displacement vectors of the relevant vibrational modes in the S_1 state for meo-OL^-.

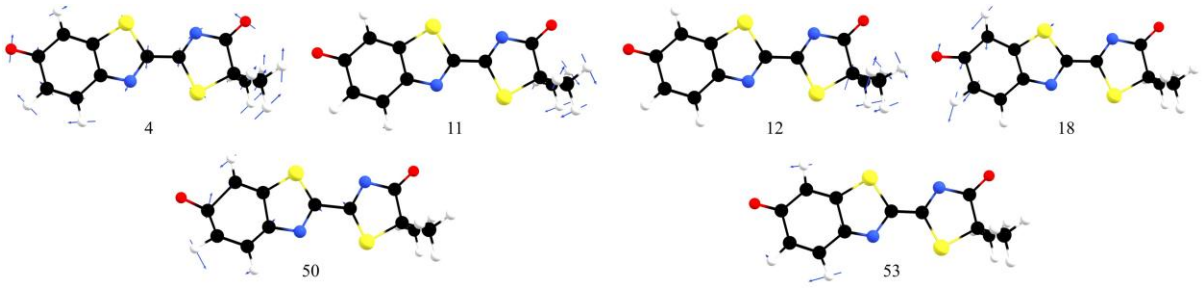

Figure S18. Scaled displacement vectors of the relevant vibrational modes in the S_1 state for dm-OL^-.

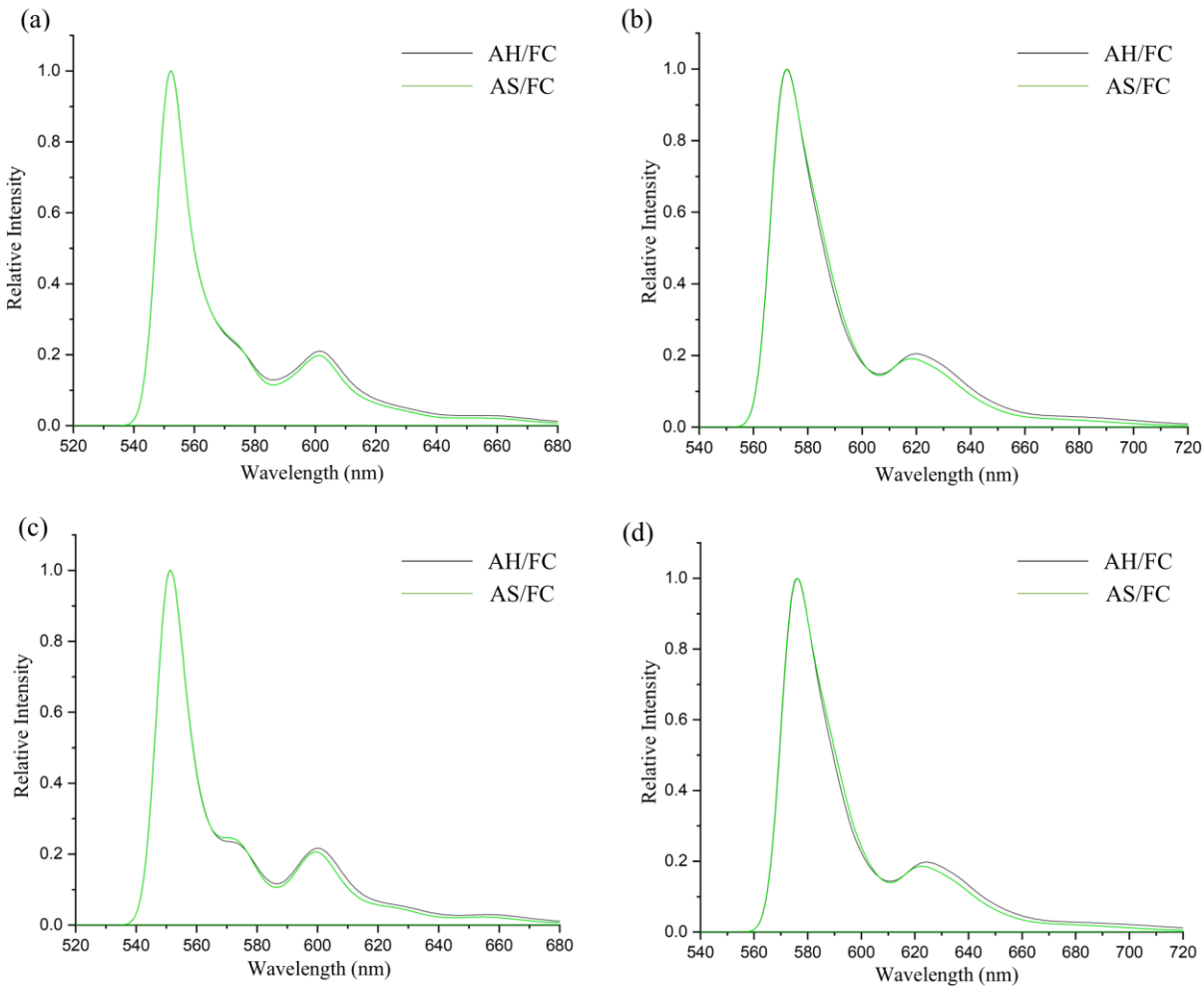

Figure S19. The comparison of fluorescence spectra of (a) phenolate-enol (b) phenolate-keto, (c) meo-OL^- and (d) dm-OL^- simulated by AS model (green line) and AH model (black line) to consider the influence of Duschinsky effect. Here, the absorption spectra simulated by the AS model is aligned with the spectra simulated by the AH model for ease of comparison.

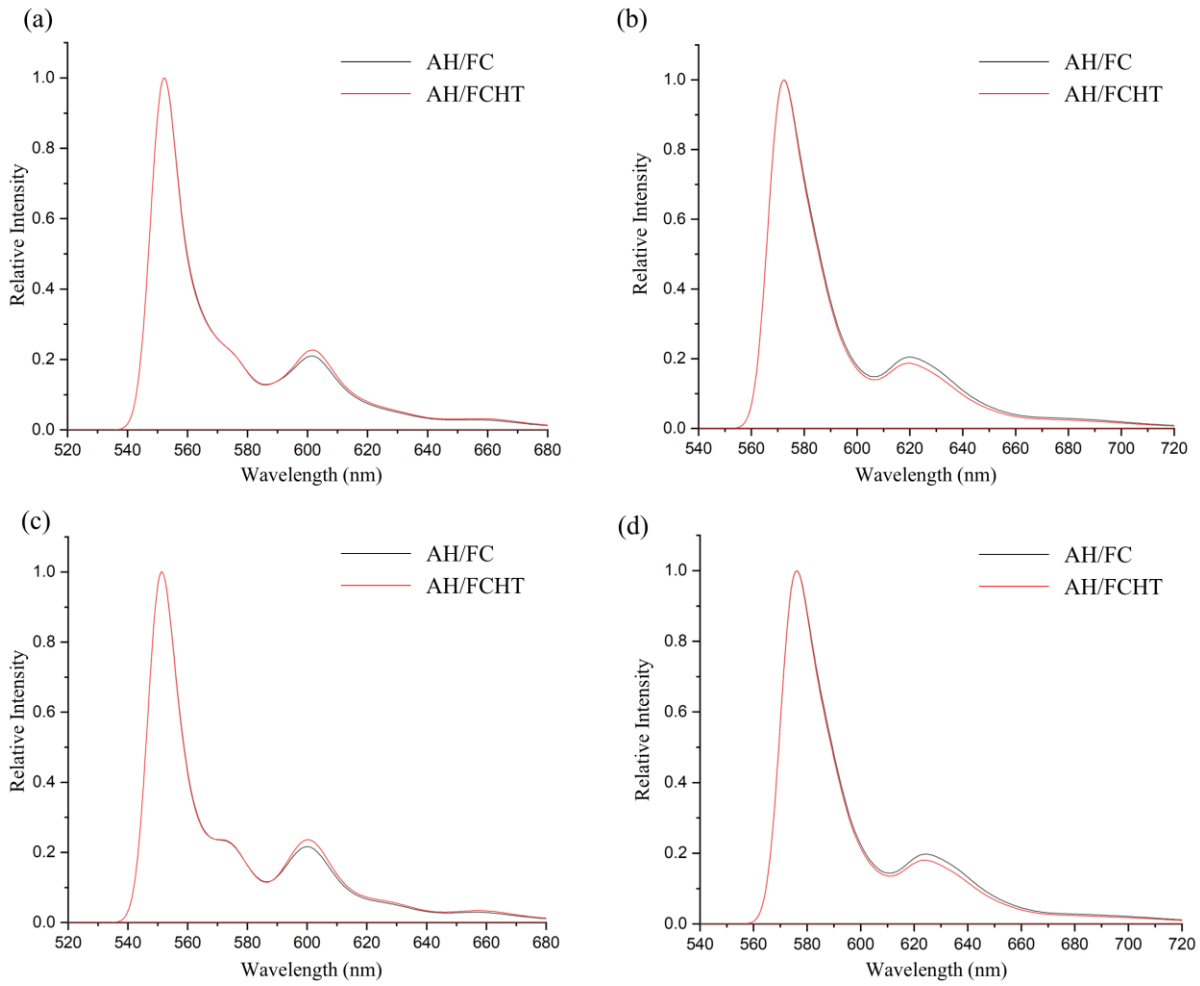

Figure S20. The comparison of fluorescence spectra of (a) phenolate-enol (b) phenolate-keto, (c) meo-OL^- and (d) dm-OL^- simulated by AH model to consider the influence of Herzberg-Teller effect. The black line represents that only FC effect is considered, while the red line represents that both FC and HT effects are considered.

The XYZ Cartesian Coordinates of Key Structures Reported (unit: Ångstrom)

S_0-state-phenolate-enol

CAM-B3LYP/aug-cc-pVTZ

C	1.961158	-0.641707	-0.000032
C	1.665156	0.746950	-0.000026
C	2.742934	1.654919	0.000038
C	4.019550	1.191924	-0.000053
C	4.356280	-0.225788	-0.000523
C	3.240903	-1.129998	-0.000136
C	-0.411613	0.014897	0.000044
H	2.527238	2.715826	0.000194
H	4.858293	1.875426	0.000087
H	3.452569	-2.189802	-0.000018
N	-2.647842	-0.939742	0.000055
C	-1.838557	0.085969	0.000004
C	-3.937015	-0.536104	0.000003
C	-4.163939	0.801448	-0.000079
O	5.545585	-0.610634	0.000198
N	0.351598	1.066533	0.000034
S	0.451160	-1.520692	0.000211
S	-2.644096	1.632012	-0.000097
O	-4.875185	-1.520811	0.000047
H	-5.103619	1.324556	-0.000122
H	-5.746140	-1.118153	-0.000004

S_1-state-phenolate-enol

CAM-B3LYP/aug-cc-pVTZ

C	-1.939898	-0.618996	0.000031
C	-1.674225	0.765370	0.000033
C	-2.772714	1.651715	-0.000039
C	-4.050147	1.175173	-0.000043
C	-4.352293	-0.242173	0.000159
C	-3.211599	-1.132325	0.000021
C	0.416087	0.042447	0.000027
H	-2.571411	2.715131	-0.000108
H	-4.897647	1.846614	-0.000137

H	-3.408011	-2.194836	-0.000015
N	2.644356	-0.965502	-0.000033
C	1.825311	0.087495	0.000017
C	3.910448	-0.562126	-0.000040
C	4.149435	0.791118	0.000002
O	-5.523405	-0.677308	-0.000141
N	-0.353888	1.124549	0.000019
S	-0.425340	-1.498842	0.000028
S	2.639124	1.637875	0.000056
O	4.872437	-1.528925	-0.000095
H	5.097236	1.300353	0.000001
H	5.731325	-1.101438	-0.000102

S_0-state-phenolate-keto

CAM-B3LYP/aug-cc-pVTZ

C	-1.947856	-0.660417	-0.000007
C	-1.626263	0.735831	-0.000012
C	-2.692127	1.672125	0.000003
C	-3.969406	1.234832	-0.000034
C	-4.328652	-0.184965	-0.000204
C	-3.232364	-1.117775	-0.000049
C	0.433594	-0.036807	0.000023
H	-2.450132	2.726739	0.000056
H	-4.799825	1.927821	0.000008
H	-3.471808	-2.171275	0.000000
N	2.617881	-1.022320	0.000026
C	1.837278	0.019801	0.000007
C	3.950420	-0.704599	0.000005
C	4.218540	0.808349	-0.000045
H	4.796536	1.067107	0.883263
O	-5.519358	-0.540167	0.000056
N	-0.330358	1.035193	0.000010
S	-0.457349	-1.560070	0.000099
S	2.612425	1.621589	-0.000046
O	4.866339	-1.496095	0.000048
H	4.796511	1.067052	-0.883385

S_1-state-phenolate-keto

CAM-B3LYP/aug-cc-pVTZ

C	-1.924379	-0.605706	-0.000057
C	-1.661950	0.776285	-0.000099
C	-2.760696	1.662684	-0.000016
C	-4.040942	1.190382	0.000012
C	-4.344499	-0.223812	-0.000275
C	-3.200800	-1.119457	-0.000006
C	0.425147	0.041784	-0.000055
H	-2.558262	2.725835	0.000062
H	-4.885708	1.864632	0.000159
H	-3.399179	-2.181453	0.000090
N	2.591510	-1.022633	0.000045
C	1.842916	0.055045	-0.000013
C	3.926343	-0.753344	0.000059
C	4.242956	0.753358	0.000022
H	4.828934	0.998838	0.882830
O	-5.508411	-0.670396	0.000277
N	-0.338095	1.125323	-0.000083
S	-0.421283	-1.487643	-0.000035
S	2.660781	1.622160	-0.000015
O	4.827760	-1.572237	0.000133
H	4.828952	0.998787	-0.882789

S_0-state-meo-OL^-

CAM-B3LYP/aug-cc-pVTZ

C	2.173255	-0.645061	0.000028
C	2.007117	0.764460	-0.000125
C	3.164629	1.567450	-0.000215
C	4.393086	0.987566	-0.000029
C	4.596789	-0.454791	0.000515
C	3.401745	-1.250875	0.000219
C	-0.129352	0.230530	-0.000110
H	3.048988	2.643874	-0.000453
H	5.291485	1.590519	-0.000171

H	3.513562	-2.325851	0.000206
N	-2.432648	-0.539230	-0.000067
C	-1.545735	0.423019	-0.000003
C	-3.691979	-0.040405	0.000179
C	-3.814314	1.310988	0.000463
O	5.744897	-0.949674	0.000010
N	0.727729	1.205401	-0.000243
S	0.587598	-1.379918	-0.000239
S	-2.236625	2.016920	-0.000094
O	-4.756736	-0.873615	0.000280
H	-4.715050	1.895542	0.000748
C	-4.470312	-2.262487	-0.000049
H	-3.899819	-2.546837	-0.883219
H	-3.899444	-2.547174	0.882771
H	-5.435712	-2.761354	0.000062

S_1-state-meo-OL^-

CAM-B3LYP/aug-cc-pVTZ

C	2.154113	-0.625425	-0.000036
C	2.015717	0.778077	-0.000041
C	3.191027	1.559960	-0.000062
C	4.418691	0.967726	-0.000086
C	4.589985	-0.471959	-0.000094
C	3.372849	-1.253172	-0.000061
C	-0.132357	0.252975	0.000015
H	3.088264	2.637324	-0.000056
H	5.324381	1.558397	-0.000103
H	3.470541	-2.329286	-0.000061
N	-2.433536	-0.564946	0.000048
C	-1.530073	0.420729	0.000040
C	-3.667175	-0.059384	0.000066
C	-3.794475	1.308153	0.000090
O	5.717057	-1.010920	-0.000123
N	0.735196	1.258471	-0.000007
S	0.564476	-1.362002	-0.000006
S	-2.222404	2.025701	0.000078
O	-4.751478	-0.871465	0.000060
H	-4.702380	1.882138	0.000108

C	-4.485155	-2.262126	0.000024
H	-3.916257	-2.553285	-0.882580
H	-3.916212	-2.553323	0.882587
H	-5.456621	-2.750057	0.000038

S_0-state-dm-OL^-

CAM-B3LYP/aug-cc-pVTZ

C	-2.566934	0.637247	0.000048
C	-2.164484	-0.737739	-0.000009
C	-3.173778	-1.734611	-0.000009
C	-4.474497	-1.372648	0.000083
C	-4.915980	0.023642	0.000265
C	-3.876169	1.018714	0.000144
C	-0.153040	0.153674	-0.000048
H	-2.870592	-2.773302	-0.000091
H	-5.263044	-2.112953	0.000062
H	-4.176707	2.056459	0.000147
N	1.960231	1.278406	-0.000046
C	1.251975	0.182860	-0.000038
C	3.307069	1.044806	-0.000057
C	3.708913	-0.450812	-0.000031
O	-6.125656	0.308677	0.000142
N	-0.853043	-0.960926	-0.000078
S	-1.131706	1.622462	-0.000080
S	2.128484	-1.354663	-0.000053
O	4.168712	1.897519	-0.000021
C	4.520662	-0.750109	1.254894
H	4.832748	-1.794209	1.274041
H	5.406062	-0.115331	1.262521
H	3.941314	-0.548539	2.153661
C	4.520712	-0.750136	-1.254916
H	5.406111	-0.115357	-1.262523
H	4.832800	-1.794236	-1.274027
H	3.941399	-0.548587	-2.153710

S_1-state-dm-OL^-

CAM-B3LYP/aug-cc-pVTZ

C	2.541194	0.586376	0.000011
C	2.203710	-0.779396	0.000025
C	3.252059	-1.724941	-0.000046
C	4.556000	-1.323381	-0.000065
C	4.936398	0.072385	0.000141
C	3.843512	1.029215	-0.000025
C	0.159946	0.067172	0.000031
H	2.991545	-2.775356	-0.000108
H	5.362707	-2.042752	-0.000167
H	4.099810	2.078757	-0.000075
N	-1.935727	1.259412	-0.000003
C	-1.256653	0.133780	0.000013
C	-3.280992	1.068521	-0.000016
C	-3.723644	-0.418482	0.000019
O	6.123118	0.454054	-0.000229
N	0.863286	-1.056006	0.000021
S	1.088147	1.548923	0.000044
S	-2.166217	-1.371150	0.000018
O	-4.130182	1.944207	-0.000015
C	-4.543532	-0.700193	-1.254121
H	-4.888017	-1.734506	-1.269891
H	-5.408019	-0.036955	-1.263362
H	-3.958205	-0.518814	-2.153298
C	-4.543497	-0.700150	1.254192
H	-5.407979	-0.036906	1.263436
H	-4.887988	-1.734460	1.270000
H	-3.958144	-0.518749	2.153347